Electronic Supporting Information

High-pressure induced a stable phase of Li_2MnSiO_4 for an effective poly-anion cathode material from simulations

Shuo Wang[a], Junyi Liu[a], Yu Qie[a], Sheng Gong[b], Cunzhi Zhang[a] Qiang Sun[c,d,a,*], and Puru Jena[e]

[a] Department of Materials Science and Engineering, College of Engineering, Peking University, Beijing 100871, China

[b] Department of Materials Science and Engineering，Massachusetts Institute of Technology，Cambridge，MA 02139，USA

[c] Center for Applied Physics and Technology, Peking University, Beijing 100871, China

[d] Key Lab of Theory and Technology for Advanced Batteries Materials, College of Engineering, Peking University, Beijing 100871, China

[e] Department of Physics, Virginia Commonwealth University, Richmond, VA 23284, USA

Structural information

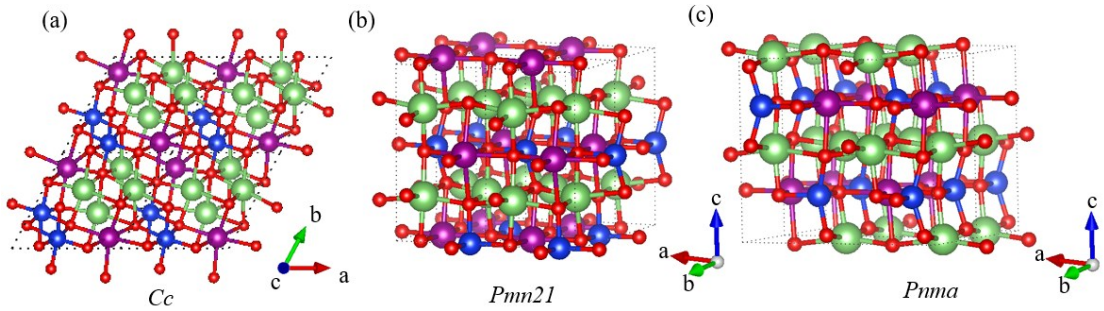

Figure S1. Geometry structures of different Li_2MnSiO_4 with space group of (a) *Cc*, (b) *Pnma* and (c) *Pmn21*.

Structural Stability

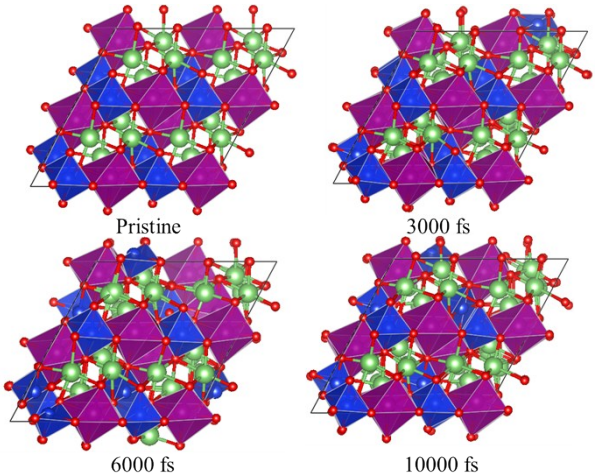

Figure S2. The snapshots of structural geometry of *Cc* Li_2MnSiO_4 extracted from AIMD simulation at 500K.

Table S1. Lattice parameters of primitive cell of predicted Li_2MnSiO_4 with space group of *Cc* after removing the pressure.

Symmetry	a=b (Å)	c (Å)	α=β(°)	γ(°)
Cc	6.00	4.94	108.79	58.16
Atom	*x*	*y*	*z*	Sites
Li1	0.84	0.61	0.86	2
	0.61	0.84	0.36	
Li2	0.37	0.61	0.84	2
	0.61	0.37	0.34	
Mn	0.11	0.84	0.33	2
	0.84	0.11	0.83	
Si	0.37	0.10	0.87	2
	0.10	0.37	0.37	
O1	0.01	0.69	0.59	2
	0.69	0.01	0.09	
O2	0.43	0.24	0.64	2
	0.24	0.43	0.14	
O3	0.24	0.03	0.11	2
	0.03	0.24	0..61	
O4	0.46	0.79	0.65	2
	0.79	0.46	0.15	

Table S2. The charge of Mn and O atoms in *Cc* $Li_{2(1-x)}MnSiO_4$ (x=0.00, 0.25, 0.5, 0.75) based on Bader Charge analysis.

$Li_{2(1-x)}MnSiO_4$	x=0.00	x=0.25	x=0.50	x=0.75
Mn1	+1.55	+1.74	+1.90	+1.95
Mn2	-1.52	+1.63	+1.90	+1.94
O1	-1.84	-1.68	-1.70	-1.52
O2	-1.84	-1.78	-1.83	-1.61
O3	-1.94	-1.79	-1.74	-1.61
O4	-1.94	-1.78	-1.61	-1.50
O5	-1.88	-1.77	-1.70	-1.51
O6	-1.88	-1.79	-1.83	-1.86
O7	-1.89	-1.85	-1.74	-1.68
O8	-1.89	-1.66	-1.61	-1.41

Table S3. Energy difference ΔE (eV) between initial and end state and migration barrier (eV) for Mn displacement to adjacent Li vacancy.

Group symmetry	*Pmn21*	*Pnma*	*Cc*
ΔE	0.53	0.46	-0.23
Migration barrier	1.10	1.06	1.48

Electronic properties

As a cathode material, the electronic conductivity is crucial to the overall battery performance, especially for charging/discharging efficiency. Usually, the poly-anion materials have large bandgap (>3eV) due to the strong bonding between polyanion groups and metal-containing polyhedrons. For instance, olivine-structure $LiFePO_4$ has a band gap of 4.1 eV[1] and shows low electron conductivity, which limits the application at low temperature. We calculate the band structure of *Cc* Li_2MnSiO_4 using GGA+U (U=6.0 eV) as shown in Figure S2, indicating that the Cc phase is a semiconductor with 3.20 eV bandgap which is comparable to those of *Pnma* (3.07 eV) and *Pmn21* (3.05 eV) phases [data from Material Project[2]]. To get more accurate result, the band

structure is also calculated using the HSE06 functional[3], which gives the band gap of 5.0 eV. The density of states suggests that the O 2p-orbital and Mn 3d-orbital mainly contribute to the states around the Fermi level, which implies the competence of redox between Mn and O during delithiation. This is different from the situations in Li_2MnO_3 and CoO_2.[4]

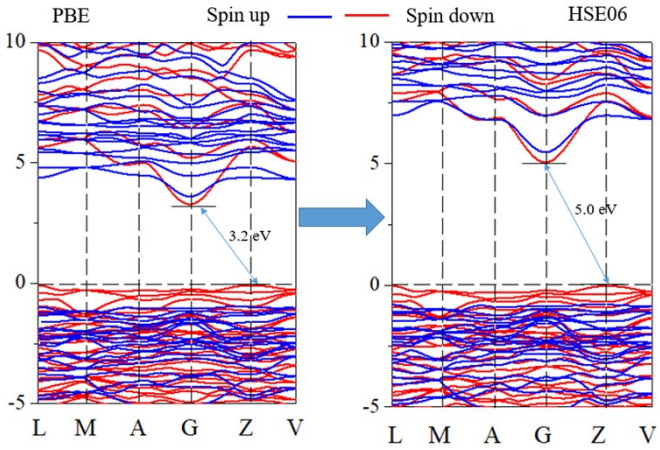

Figure S2. Band structures of *Cc* Li_2MnSiO_4 calculated using (a) PBE and (b) HSE06 functional.

Ionic Diffusion

For CI-NEB calculation, two different supercells are used: 2×2×3 (256 atoms; a=b=12.0 Å, c=14.8 Å) and 2×2×2 supercell (128 atoms; a=b=12.0 Å, c=9.9 Å), both give very similar results for the energy barrier as shown in Figure S3, indicating that 2×2×2 supercell can be used for reducing the computational cost. To accelerate the ion-hopping process, temperature is elevated from 700K to 2500K. Thermalization over 4-ps with a time-step of 2 fs is carried out before diffusion calculation.

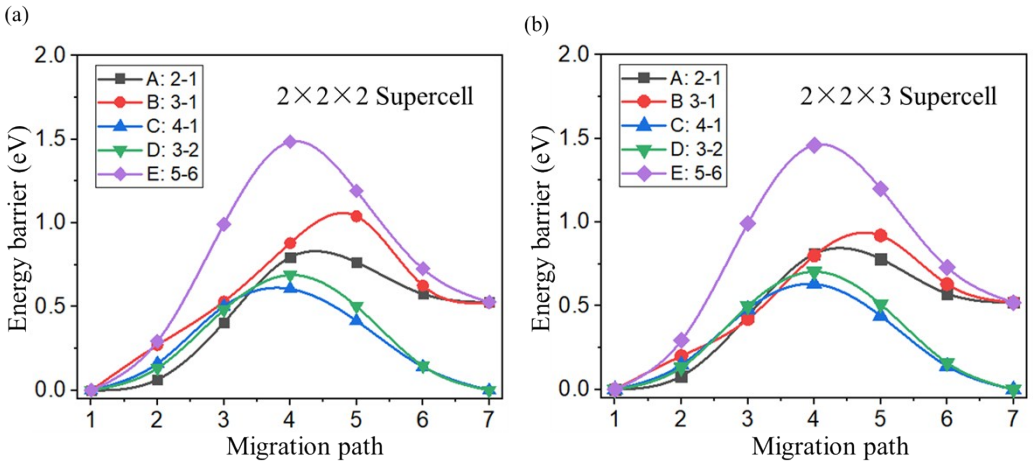

Figure S3. Energy barrier of Li diffusion in *Cc* Li_2MnSiO_4 in (a) a 2×2×2 supercell and (b) a 2×2×3 supercell

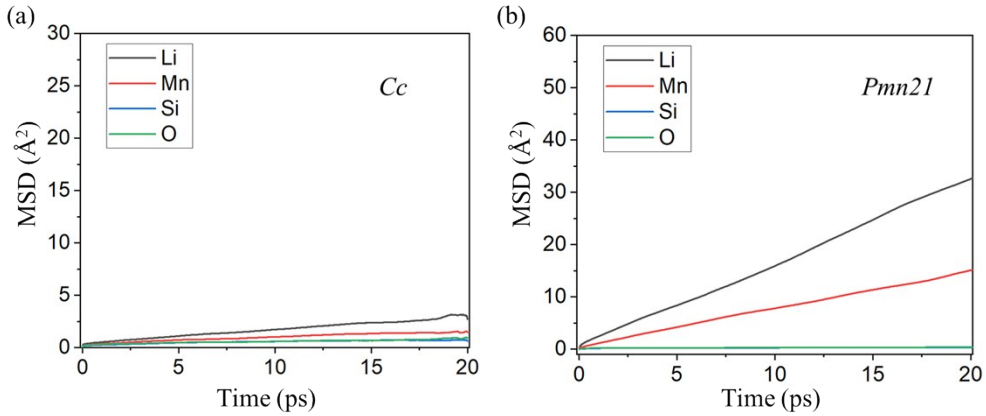

Figure S4. MSD for Li, Mn, Si, O atoms as a function of AIMD simulation time at different at 2000K for Li_2MnSiO_4 of (a) Cc phase and (b) Pnm21 phase. Same carrier concentration is used that 8 vacancies are introduced into a 2×2×2 supercell both for predict and experimental phases.

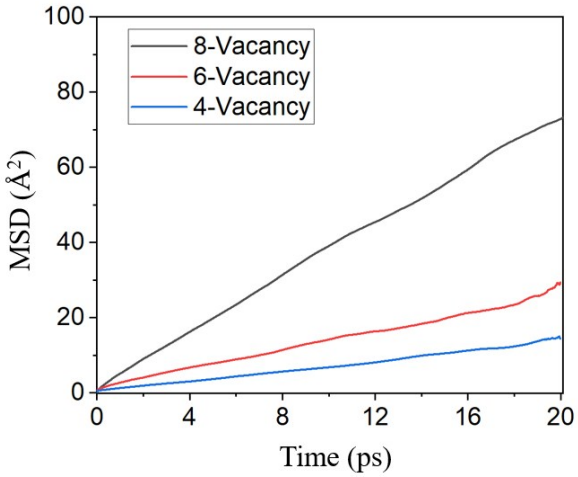

Figure S5. MSD of Li ion diffusion in a 2×2×2 supercell of *Cc* Li_2MnSiO_4 with different carrier concentration by introducing 8, 6 and 4 vacancies.

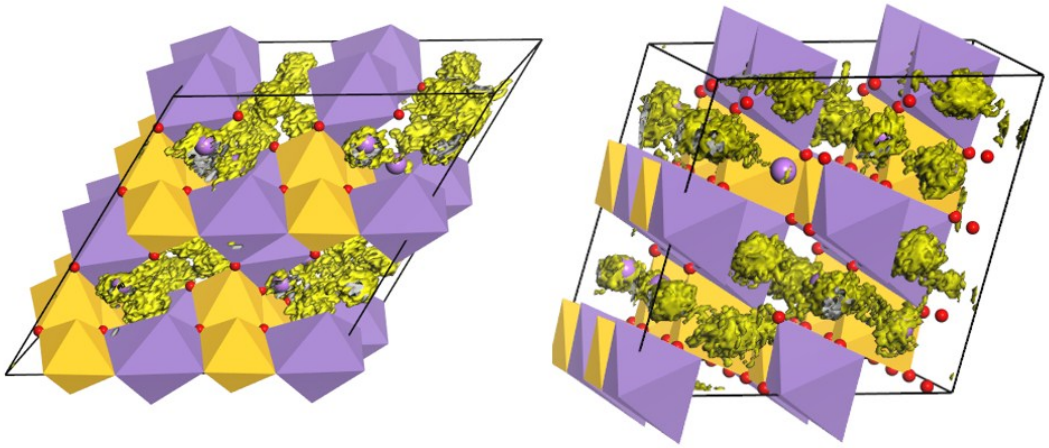

Figure S6. Projection of Li trajectories (yellow) in different views at 1500 K in a 2×2×2 supercell

of *Cc* Li_2MnSiO_4.

References

[1] A. K. Padhi, K. S. Nanjundaswamy, and J. B. Goodenough, Journal of the electrochemical society **144**, 1188 (1997).

[2] A. Jain *et al.*, Apl Materials **1**, 11002 (2013).

[3] J. Heyd, Journal of Chemical Physics **118**, 8207 (2003).

[4] S. Wang, J. Liu, and Q. Sun, Journal of Materials Chemistry A **5** (2017).